

ON-SHORE HYDRAULIC LOADS: EARTHQUAKE EXCITED TSUNAMIS

Angelo Emmanuel Thurairajah¹

ABSTRACT

Loads on building structures exposed to the forces of tsunamis excited by marine earthquakes are investigated. A tsunami is traced through the phases of source, energy input to water, deep ocean wave, wave approaching shore, dry-land run-up, inundation depth and load. Inundation depths are determined using generation, propagation and run-up models available in the literature. Inundation depths are converted to pressures and loads at the beachfront and inland zones using hydraulic models. A simple model is proposed for hydraulic pressures on walls and piles/columns of an on-shore structure following parametric studies and comparisons with unpublished field data.

Introduction

Loads generated by tsunamis due to excitation of marine earthquakes are investigated. Most of such tsunami causing earthquakes are historically recorded when one tectonic plate subduct over the other. A tsunami is traced through the following phases: Source, Energy to water, Ocean wave, Wave approaching shore, Dry-land run-up, Inundation Depth.

Part of the energy generated from a tsunami earthquake transforms into wave energy. This energy is transmitted from fast moving small amplitude deep-ocean waves to slower but taller waves approaching the shore. On shore these waves usually run as bores without breaking, generating substantial forces on the objects they come in contact with.

Inundation depths at beach front and inland zones from a coastline are determined using generation, propagation and run-up models available in the literature. Inundation depths are converted to pressures and loads using a hydraulic model.

A simple model is proposed for hydraulic pressures on walls and piles/columns of a structure based on parametric studies and observed field data. Approximate inundation depths are determined for far-field and near-field tsunamis. Scour depths of footings are also discussed. USGS/SI units are used typically throughout this manuscript.

¹Senior Structural Engineer, URS Corp, Melbourne, Australia

Marine Earthquake

Marine earthquakes are the source of majority of tsunamis ($\approx 90\%$), but submarine landslides and pyroclastic (volcanic) flows also have created high intensity tsunamis. Such earthquakes are identified by the moment magnitude (M_w) scale and the earthquake energy (E_s) in generating a tsunami. Energy trapped in a tsunami (E_t) is found to be dependent on the earthquake moment magnitude (M_w). The empirical relationships are (Murty 1977):

$$E_t \approx E_s/10 \quad (1)$$

$$\log E_t = 10.3 + 1.5M_w \quad (2)$$

Tsunami earthquake energy is defined as major ($M_w = 9$) and minor ($M_w = 7.5$) moment magnitudes for purposes of estimating their effects.

Studies of magnitudes and their effects are available for US (Garcia & Houston 1976) and Japan & the Pacific Ocean (Horikawa & Shuto 1981) and the 2004 Indian Ocean tsunami.

Ocean Wave

Part of the energy from the source is transferred from impulse excitation to potential energy change of water in its vicinity to create waves. In the ocean the tsunami appears as a small amplitude oscillatory long wave rapidly traveling towards the shore.

Wave in the ocean approximately satisfies linear Airy wave theory with celerity (c) and wave length (L) at depth (d) for $d \ll L$ is given by (where g = gravity):

$$c = [(gL/2\pi) \cdot \tanh(2\pi d/L)]^{1/2} \approx (gd)^{1/2} \quad (3)$$

Wave energy in a wave length is (H = wave height & ρ = density of water):

$$E_t = \rho g H^2 L / 8 \quad (4)$$

Typical characteristics of a tsunami in the ocean are (Mader 1988): amplitude = 0.5m to 1m, period = 10min to 30min & wave length = 200km to 600km.

Near Coastal Wave

As the wave approaches the coast the amplitude increases and the wave length decreases. The wave undergoes transformation due to shoaling on a sloping bed near the shore. Smaller waves called fore-runners arrive first before the tsunami. Withdrawal of water at coast may be observed if a trough reaches first.

Tsunamis amass several magnification effects (Bryant 2001). Edge waves can form along the beach increasing the amplitude. Bays could generate resonance; islands & cliffs could create significant local effects.

Tsunami is observed as a solitary wave or a bore offshore and a bore or soliton onshore.

Approximately 90% energy is lost as the tsunami reaches the shore by refraction, shoaling, bottom friction, coriolis effect etc (Murty 1977). Assuming the tsunami energy reaching the shore (E_{ts}) is dependent upon the energy received at the source (E_t) and the epicenter distance from the shore (R), an empirical relationship can be proposed as:

$$E_{ts} \approx \alpha \cdot E_t; \text{ where } \alpha = [E_t/(R+100)]^{1/2}/15000 \quad (5)$$

Energy per wave length in a solitary wave is (Muir Wood 1981):

$$E_{ts} = 8\rho g \cdot (Hd/3)^{3/2} \quad (6)$$

Wave celerity of the solitary wave approaching shore is (Mader 1988):

$$c = (gd)^{1/2} \cdot [1 + (H/2d) - 0.15(H/d)^{1/2}] \quad (7)$$

Wave height (H_s) near the shore could be determined from equations 1, 2, 5, 6 & 7 and in deep ocean (H_0) with equation 4. A major and a minor Tsunami on 2 bed-slopes are presented in Figures 1a and 1b respectively. Reducing wavelengths and increasing amplitudes are observed as the tsunami approaches the shore. Off-shore amplitudes are larger with narrower wavelength for the tsunami on shallower bed slope, but the differences tend to cease at shore.

Wave height at shore (H_s) are 2m & 5.8m with $R = 2000\text{km}$ (far-field) for minor and major tsunamis respectively. H_s increase to 3.2m & 8.7m with $R = 100\text{km}$ (near-field). $T = 900\text{second}$ is used.

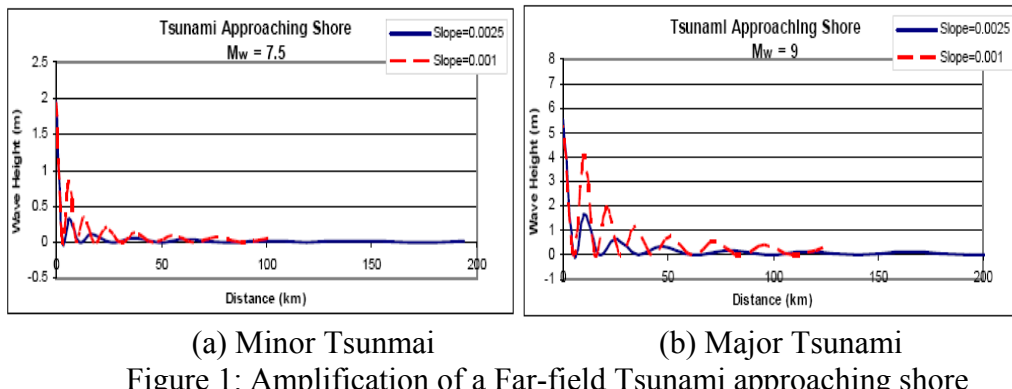


Figure 1: Amplification of a Far-field Tsunami approaching shore

Wave height at shore ' H_s ' is (Garcia & Houston 1974) given below, where x = distance of ' H ' from shore & J = Jacobian. Results are similar to that predicted by Figure 1:

$$H_s = H/J_0(2(kx)^{1/2}) \text{ with } k = (2\pi/T)^2 x_0/(gH) \quad (8)$$

Coastal Run-up

Classical Keller & Keller/Shuto's formula of run-up height (H_r) to incident wave height at shore (H_s) has been experimentally verified with two types of run-up (Togashi & Iwasaki 1976). Logarithmic relationship is shown approximately on Figure 2. 'l' & 'L' denote length of bed slope

and wave length respectively (where $U = 4\pi l/L$).

$$H_r/H_s = [J_0^2(U) + J_1^2(U)]^{1/2} \quad (9)$$

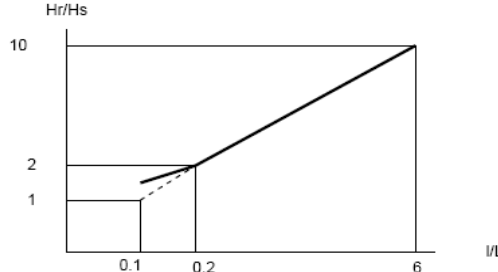


Figure 2: Run-up/Shore Height to Bed-slope/Wave Length

In the first type, wave breaks offshore due to shoaling transformation and runs as a disturbed progressive breaker noted in Figure 3a as;

$$(g/d)^{1/2} \cdot T/2 < 200 \text{ & } H/L < 0.001 \quad (10a)$$

In the second type, there is little shoaling and therefore no breaking. This mode is observed in the 2004 tsunami. The front takes disturbed form of a transitory breaker or runs as undisturbed non-breaking partial claptois noted in Figure 3b as;

$$(g/d)^{1/2} \cdot T/2 > 200 \text{ & } H/L < 0.001 \quad (10b)$$



Figure 3: Typical Breaker and Non-breaker Run-ups

Consideration of backwash results in smaller run-ups (Chu & Abe 1981). Also, the wave height at shore needs to be about 3 times the inundation depth (h) for the wave to break (Pelinovsky 1998). With a range of:

$$H_s < H_r < 5.4H_s \quad (11)$$

Inundation Depth

Approximate inundation depths for far-field and near-field tsunamis are determined for beachfront and inland zones. Beachfront zone is ' L_1 ' long from the coastline and inland zone is ' L_2 ' long following this. If 'R' is the distance of epicenter from shoreline;

$$L_1 = 2000/R^{0.25}; L_2 = 2L_1 \quad (12)$$

Assuming the dry-land beach and adjacent area slopes are small, it could be seen that the inundation depth (h) is closely related to the run-up height (H_r), wave height at shore (H_s) and distance from shore (x).

Design inundation depth ‘h’, accounting for backwash is:

$$h = 3H_s \text{ for Beachfront; } h = H_s \text{ for Inland} \quad (13)$$

Table 1 summarizes the inundation depths and zones for far-field and near-field major/ minor tsunamis investigated in this manuscript. The magnitudes of the inundation depths are similar to those observed in Indonesia and Sri Lanka during the 2004 tsunami.

Table-1: Design Inundation Depth

Proximity	Zone	EQ	Depth
Near-Field (R = 100km)	Beachfront (L ₁ =)	Major	26
		Minor	10
	Inland (L ₂ =)	Major	9
		Minor	3
Far-Field (R = 2000km)	Beachfront (L ₁ =)	Major	17
		Minor	6
	Inland (L ₂ =)	Major	6
		Minor	2

Local magnification effects could be accounted by increasing the inundation depths and extents of zones given above by 50% where edge wave effects could be expected and by 100% in bays, harbors, river deltas, estuaries, lees of islands etc.

Load Models

Various models predicting hydraulic forces due to tsunami are presented in this section. Static & dynamic components of wave loads offshore and onshore from the shore-line due to the impact of breaking wave are illustrated in Figure 4 (Muir Wood 1981).

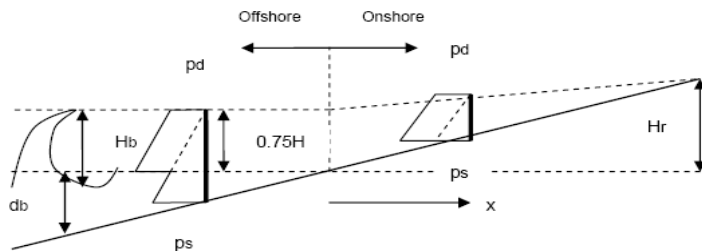


Figure 4: Offshore and Onshore Hydraulic Pressures

Tsunami bore velocity & pressure at inundation depth of ‘h’, with $u = 1.83(gh)^{1/2}$ & $C_d = 1.2$ and $p = p_s + p_d$ is given by (Murty 1977):

$$p_d = \frac{1}{2} \rho C_d u^2 \text{ (uniform distribution); } p_s = \rho g h \text{ (triangular distribution)} \quad (14)$$

Bore front velocity ‘u’ on dry bed of slope ‘S’ with friction ‘f’ at distance ‘x’ from the shoreline (Togashi 1976):

$$u = (u_s - Bx)^2 \quad (15)$$

u_s = velocity at the shoreline & $B = 2(S + f/a^2)/[(1+a)(1+2a)]$ with $a = \frac{1}{2}$
 $u = 0$ when reaching maximum run up and $x = (H_r - H_s)/S$

$$S = 0.0025, f = 0.01, H_r = 12m \text{ & } H_s = 3m \text{ gives } u_s = (3.4gh)^{1/2}$$

$$S = 0.001, f = 0.03, H_r = 6m \text{ & } H_s = 2m \text{ gives } u_s = (16.4gh)^{1/2}$$

At $x = 10m$ from shore these velocities reduce to $(0.34gh)^{1/2}$ and $(0.88gh)^{1/2}$ respectively.

Design and Construction guideline of buildings in the coasts of USA outlines loads, bore velocity, load combinations etc (FEMA 2000).

$$\text{Static pressure (triangular distribution)} p_s = \rho gh \quad (16.1)$$

$$\text{Dynamic (drag) pressure } p_d = \frac{1}{2} C_d \rho u^2 \quad (16.2)$$

$$\text{Wave breaking pressure } p_b = C_b \rho gh \text{ for piles } (1.1C_p + i) \rho gh \text{ for walls} \quad (16.3)$$

Velocity $u = h/t$ (lower limit), $(gh)^{1/2}$ & (upper limit) & $2(gh)^{1/2}$ (extreme- tsunami);

Triangular/uniform dynamic pressure distribution for $u <$ or $> 3m/s$ respectively; $C_d = 2$ for rectangular & 1.2 for circular section. Uniform wave breaking pressure distribution; $C_b = 2.25$ for rectangular and 1.75 for circular sections; $i = 2.41$ & 1.91 for water on one-side & both-sides; $C_p = 2.8$ for general and 3.2 for critical facilities.

$$\text{Force due to impact of a floating object } F_i = m_a \cdot u_a / t \quad (16.4)$$

m_a = mass (450kg) & u_a = velocity and $t = 1, 0.5$ & 0.1 sec for wood, steel & concrete.

Load combination to establish appropriate design actions are;

For piles: (i) p_b on all + F_i on one, or (ii) p_b on front row + p_d on others + F_i on one

For walls: (i) $(p_b + p_d)$, for coastal, and (ii) $(p_s + p_d)$, for inland buildings $\quad (16.5)$

A parallel source from Japan (SDMBTR 2005) provides expressions to determine loads. Pressure distribution due to tsunami is based on the model proposed by Asakura for the case of solition without break-up.

Base pressure against a wall as in Figure 5a with triangular distribution is given by (where pressure on the front & rear walls are ' p ' and sides are ' $0.5p$ ' - plan on Figure 5(c)):

$$p = 3\rho gh \quad (17.1)$$

Base pressure at an elevated wall as in Figure 5b is,

$$p = 3\rho g(hh')^{1/2} \quad (17.2)$$

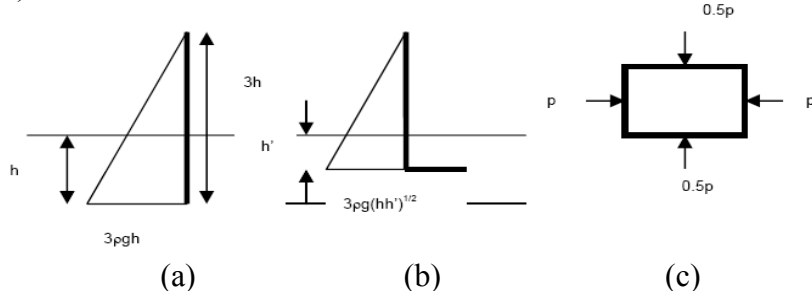


Figure 5: SMBTR Pressure Distribution

Total pressure at base is,

$$p = 3\rho gh + 2.4\rho gh \quad (17.3)$$

Base pressure distribution due to soliton break-up is shown in Figure 6 (SDMBTR 2005):

$$\text{Drag pressure, } p_d = \frac{1}{2} C_d \rho u^2; C_d = 2.05 \quad (18.1)$$

$$\text{Inertial pressure, } p_m = C_m \rho (du/dt)h \text{ where } du/dt \text{ is gradient; } C_m = 2.19 \quad (18.2)$$

$$\text{Impulse pressure, } p_t = \frac{1}{2} C_t \rho u^2; C_t = 3.6 \cdot \tan\beta, \text{ where } \beta = \text{incident angle} \quad (18.3)$$

$$\text{Total pressure, } p = p_d + p_m + p_t \quad (18.4)$$

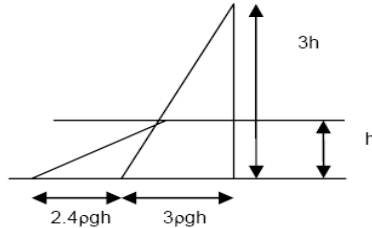


Figure 6: Asakura's Model for Soliton break-up

Scour depth (d_s) of footings at inundation depth (h) for width (w) is (FEMA 2000):

$$\begin{aligned} \text{For strips: } d_s &= h \{2.2(w/h)^{0.65} [u/(gh)^{1/2}]^{0.43}\} K = (4wh^{1/2})^{0.65} \text{ for } K = 2.2 \text{ & } u = gh^{1/2} \\ \text{For piles: } d_s &= 2w \end{aligned} \quad (19)$$

Uplift effects on the buildings could be assumed to be primarily due to buoyancy, ignoring hydrodynamic uplift (ρ = density of tsunami water & V = volume of submerged structure):

$$\text{Uplift } U = 1.2\rho g V \quad (20)$$

Conclusion

Inundation depth with respect to distance from coastline and size of tsunami are derived. Inundation depth is the basic input to derive the hydraulic loads.

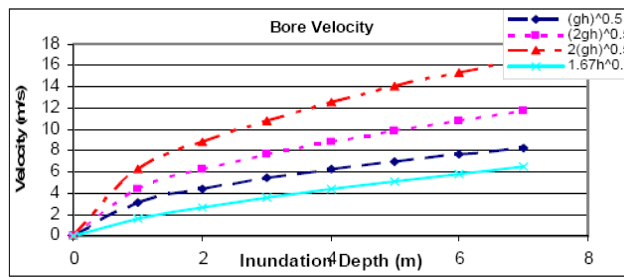


Figure-7: Bore Velocity Distribution

There is no agreement between the various methods listed above as to the hydraulic pressure components, design velocity or pressure coefficients adopted. Also a breaking or non-

breaking wave could make further difference.

Figure 7 shows bore velocity distribution with inundation depth. Limited field data available suggests a value of $(2gh)^{1/2}$ in the beachfront zone. Equation 15 indicates rapid decay of the peak velocity. Velocity is not likely to exceed $(gh)^{1/2}$ in the inland zone.

Figure 8 illustrates the loads calculated on a '3h' minimum high wall using SMBTR equation 17.1. Also included are effects of soliton break-up as in equations 17.3 and 18.4.

For walls shorter than '3h', the model recommends curtailing the pressure distribution outside the wall as in equation 17.2.

Hydrodynamic loads induced by a tsunami consists of inertial, dynamic/drag & impulse/ shock in SDMBTR models and dynamic/drag & wave breaking (including static) in the FEMA model. Impulse/shock or wave breaking could account to about 50% or more of the total loading. Since most bores run inland without breaking, these models may over-estimate the inland on-shore tsunami loads.

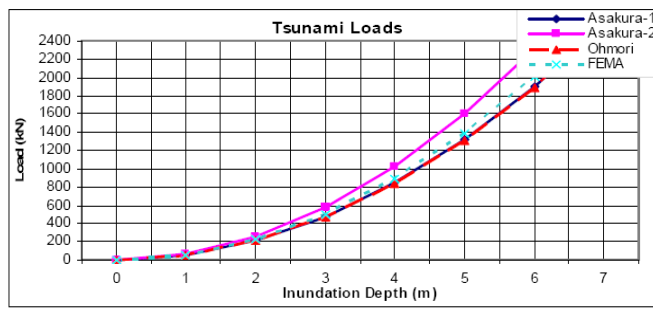


Figure-8: Tsunami Load on Wall

An alternative model is suggested as shown in Figure 9. Pressure distribution consists of static, dynamic/drag and impulse/shock components due to tsunami flow around a building in the Beachfront Zone are:

Triangular static pressure distribution at base $p_s = \rho gh$

Uniform dynamic/drag pressure $p_d = 1.25\rho gh$, $u = (1.67gh)^{1/2}$ and $C_d = 1.5$.

Impulse/shock pressure $p_t = 0$ to $1.75\rho gh$ to $0.75\rho gh$ from 'h' above inundation depth to the base (derived from equation 18.3).

Total pressure, $p = p_s + p_d + p_t$ (21)

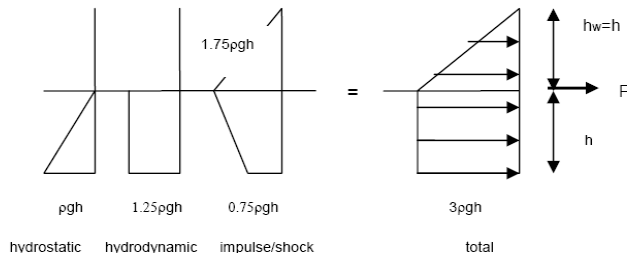


Figure 9: Proposed Hydraulic Pressure Distribution

The total pressure becomes constant ' $3\rho gh$ ' within the inundation depth 'h' and decreases to '0' at 'h' above the surface. The model gives similar force 'Fi' as the Asakura-1 & Ohmori of

SMBTR and FEMA as illustrated in Figure 8.

These pressures are applicable if the design exposed surface area is greater than 24m^2 and double these values should be used for localized pressures on elements of area less than 6m^2 . Linear interpolation could be used for intermediate values.

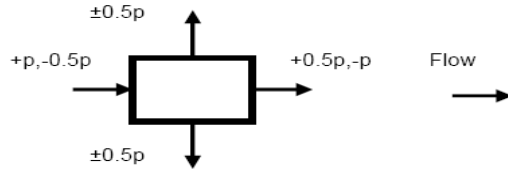


Figure-10: Hydraulic Loads on an Idealized Building

Plan showing pressure distribution around the perimeter of a typical rectangular building is shown in Figure 10. Loads are to be calculated as the sum of pressures against the all area.

Piles may be designed for a uniform pressure distribution of ' 3pgh ' for square sections and ' 2pgh ' for circular sections. Also piles directly exposed to impact from debris should be checked for half the above loads + impact load as given in FEMA equation 16.4. Debris velocity u_a' = $\frac{2}{3}u_a$ is recommended.

Velocity $u = (gh)^{1/2}$ and coefficient $C_d = 1.5$ are appropriate for tsunami runs inland, which reduces to constant ' ρgh ' dynamic/drag pressure within the inundated depth. Impulse/shock pressure varies from 0 to ' ρgh ' to 0 from ' $h/2$ ' above the surface to base. $\frac{2}{3}$ of the hydraulic loads and $\frac{1}{2}$ the debris load calculated for a beachfront zone may be used for inland zones.

Soil scour at footings are common cause of building failures as witnessed in the 2004 tsunami. FEMA recommendation for piles is adequate but a new proposal is suggested for strip footings in beachfront zone as below and illustrated in Figure 11 for $w = 0.6\text{m}$;

$$\text{Footing depth } d_s = (wh+1)^{0.65} \quad (22)$$

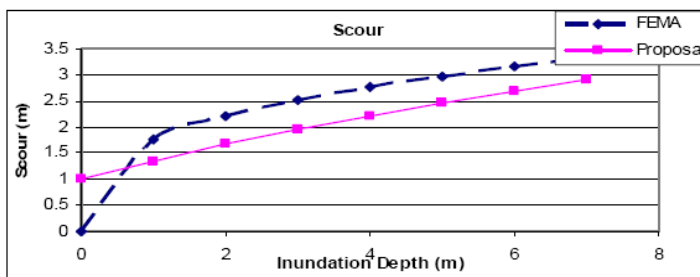


Figure 11: Footing Scour Depths for Beachfront Zone ($w=0.6\text{m}$)

Scour depths extend lengths of ' $1.5d_s$ ' from the corners of the buildings. Minimum ' d_s ' of 0.8m is recommended. In sandy soils depths shall be increased by 50%. $\frac{2}{3}$ of beachfront zone design scour depth may be used for inland zone.

Reduced footing sliding resistance due to buoyancy also needs to be considered. Added with scouring, reduced sliding resistance could result in of structural failure of buildings.

References

- Horikawa K. & Shuto N., 1981, *Tsunami Disasters and Protection Measures in Japan*, Tsunamis: Their Science and Engineering, 10th IUGG International Tsunami Symposium, Sendai-shi/Miyagi-ken, Japan.
- Murty T.S., 1977, *Seismic Sea Waves: Tsunamis*, Bulletin of the Fisheries Research Board of Canada- No. 198, Department of Fisheries and the Environment, Scientific Information and Publishing Branch, Ottawa, Canada.
- Mader C.L., 1988, *Water Wave Theory*, Los Alamos series in basic and applied sciences, University of California Press, Berkeley, USA.
- Muir Wood A.M., 1981, *Coastal Hydraulics*, 2nd edition, Macmillan Publishers, London, UK.
- Garcia A.W. & Houston J.R., 1974, *Tsunami Run-up Predictions for Southern California Coastal Communities*, NOAA-JTRE, Tsunami Research Symposium, International Union of Geodesy & Geophysics, Wellington, New Zealand.
- Togashi H., 1976, *Study on Tsunami Run-up and Countermeasure*, PhD Thesis, Tohoku University, Sendai, Japan.
- Chu K.K. & Abe T., 1981, *Tsunami Run-up and Backwash on a Dry Bed*, Tsunamis: Their Science and Engineering, 10th IUGG International Tsunami Symposium, Sendai-shi/Miyagi-ken, Japan.
- Bryant E., 2001, *Tsunami: The Underrated Hazard*, Cambridge University Press, London, UK.
- Pelinovsky E. & Troshina E., 1998, *Run-up of Tsunami Waves on a Vertical Wall in a Basin of Complex Topography*, Physics and Chemistry of the Earth, Monash University, Australia.
- Abe K., 1993, *Estimate of Tsunami Run-up Heights from Earthquake Magnitudes*, Tsunami: Progress in Prediction, Disaster of Japan Prevention and Warning, 16th International Tsunami Symposium, Wakayama-shi, Japan.
- Federal Emergency Management Agency (FEMA), 2000, Chapter11: Determining Site-Specific Loads, FEMA Coastal Construction Manual, USA.
- Building Technology Research Institute, 2005, *Proposed Structural Design Method of Buildings for Tsunami Resistance (SDMBTR)*, The Building Center, Japan.
- Thurairajah A., 2005, *Structural Design Loads for Tsunamis*, Monash University, Australia.